Novel osmium-based electrocatalysts for oxygen reduction and hydrogen oxidation in acid conditions

J. Uribe-Godínez [a], R.H. Castellanos [b], E. Borja-Arco [a],
A. Altamirano-Gutiérrez [a], O. Jiménez-Sandoval [a,*]

[a] Centro de Investigación y de Estudios Avanzados del Instituto Politécnico Nacional (Cinvestav), Unidad Querétaro,
Apartado Postal 1-798, Querétaro, Qro. 76001, Mexico
[b] Centro de Investigación en Ciencia Aplicada y Tecnología Avanzada-Querétaro, Av. Cerro Blanco No. 141,
Col. Colinas del Cimatario, Querétaro, Qro. 76090, Mexico

Abstract

In this work, novel osmium electrocatalysts for oxygen reduction and hydrogen oxidation in $0.5\,M\ H_2SO_4$, have been developed. The syntheses were performed by thermolysis of $Os_3(CO)_{12}$ and $Os_3(CO)_{12}$/Vulcan®, in two reaction media, N_2 (in the absence of solvents) and n-octane, in order to evaluate the effect of these parameters on the electrocatalytic activity of the new materials. In the solvent-free pathway, different reaction temperatures (in the 120–320 °C range) and times (5, 7 and 10 h) were explored; the syntheses in n-octane were done at reflux temperature, for 30 and 72 h. The products were characterized structurally by FT-IR spectroscopy, X-ray diffraction and scanning electron microscopy, and electrochemically by room temperature rotating disk electrode measurements, using cyclic and linear sweep voltammetry. Some materials prepared in both reaction media can efficiently perform the hydrogen oxidation and/or oxygen reduction reaction, i.e. those prepared by pyrolysis of $Os_3(CO)_{12}$/Vulcan® in N_2, at 180 °C/7 h, 320 °C/5 h, 320 °C/7 h and 320 °C/10 h, as well as the materials synthesized in n-octane (from both Os precursors); the latter, in addition, have the important property of being tolerant to carbon monoxide to some extent, in contrast to platinum, which is easily deactivated even by traces of CO.
© 2007 Elsevier B.V. All rights reserved.

Keywords: Osmium; Electrocatalyst; Oxygen reduction; Hydrogen oxidation; Polymer electrolyte fuel cell

1. Introduction

The oxygen reduction and hydrogen oxidation reactions (ORR and HOR, respectively) are of great interest for the development of polymer electrolyte fuel cells (PEFC), an important alternative energy source. In such devices, hydrogen is oxidized at the anode and oxygen is reduced at the cathode, with the production of electricity and water; these reactions, however, need to be catalyzed, usually by noble metal nanoparticles; platinum is the most widely used electrocatalyst for PEFC, however, its easy deactivation by species such as carbon monoxide results in the need of using costly, highly pure hydrogen; if carbon monoxide

tolerant catalysts were available, on the other hand, hydrogen produced from hydrocarbon reforming processes could be a practical, economically viable fuel feed for PEFC [1–4]. The rate of the oxygen reduction reaction at the cathode, on the other hand, is still low at Pt catalysts, which results in a performance capacity loss in PEFC. Hence, the development of new materials with catalytic properties to perform oxygen reduction and hydrogen oxidation is presently a challenge of great technological importance. Transition metal based materials are promising candidates for this purpose; ruthenium based materials, for example, have proved to perform the ORR in acid media [5–7], as have some Fe and Co nitrogenated systems [8–10]; Ru/C catalysts modified with iron phenanthroline complexes, have been also used [11]. As regards osmium, although some Pt–Os alloys [12] and Os-modified Pt surfaces [13] have been reported as active materials for hydrogen and methanol oxidation, to the

* Corresponding author. Tel.: +52 442 4414903; fax: +52 442 4414938.
E-mail address: ojimenez@qro.cinvestav.mx (O. Jiménez-Sandoval).

best of our knowledge, electrocatalysts based solely on osmium for the ORR have been only reported by one of the authors [14–16]; such materials, prepared in 1,2-dichlorobenzene, are also tolerant to methanol, thus being potential candidates to be used as cathodes in direct methanol fuel cells (DMFC) as well [16]. In this work, we report new osmium materials, prepared in *n*-octane and by a solvent-free route (in an N_2 atmosphere), which are able to perform the oxygen reduction reaction in 0.5 M H_2SO_4. Some of these novel materials can also perform the hydrogen oxidation reaction, even in the presence of carbon monoxide, unlike platinum. This is also the first report, as far as we know, of a non-alloy type osmium electrocatalyst for this reaction.

2. Experimental

2.1. Preparation and characterization of the electrocatalysts

The synthetic procedure was as follows: 0.066 mmol of triosmium dodecacarbonyl [$Os_3(CO)_{12}$, Strem Chemicals] and 4.99 mmol of Vulcan® (XC-72R, Cabot) were mixed in 100 ml of *n*-hexane (J. T. Baker); the mixture was then heated at 60 °C for 24 h, and the solvent removed by evaporation. The resulting $Os_3(CO)_{12}$/Vulcan® mixture, as well as *untreated* $Os_3(CO)_{12}$, were used as precursors for the preparation of the new materials by the two following general routes: (A) 50 ml of *n*-octane (Aldrich; bp 125 °C) were added to 40 mg of $Os_3(CO)_{12}$/Vulcan® and the mixture kept under reflux conditions for 30 h. The reaction was also performed with $Os_3(CO)_{12}$, for 72 h. The products were centrifuged and washed with diethyl ether (J. T. Baker) and dried at room temperature. (B) Pyrolysis of 40 mg of $Os_3(CO)_{12}$/Vulcan® on a Lindberg/Blue tubular furnace, in N_2 atmosphere, at 120, 180, 240, 280 and 320 °C, for 5, 7 and 10 h. The products (blackish powders in all cases) were characterized by infrared spectroscopy, on a Nicolet-Avatar 360 spectrometer (with the samples as FT-IR grade KBr discs), by X-ray diffraction, on a Rigaku D/max-2100 diffractometer (Cu Kα_1 radiation, 1.5406 Å) and by scanning electron microscopy on a Philips XL30ESEM microscope.

2.2. Electrode preparation

The electrodes for the rotating disk electrode (RDE) measurements were prepared as follows: for the catalysts synthesized from the $Os_3(CO)_{12}$/Vulcan® mixture, 2 mg of material and 25 μl of a 5% Nafion®/isopropanol solution (ElectroChem) were mixed in an ultrasonic bath for 5 min; 5 μl of the resulting slurry were deposited on a glassy carbon electrode and dried in air; a similar procedure was followed for the catalysts prepared from $Os_3(CO)_{12}$, except that 1 mg of catalyst and 1 mg of Vulcan® powder were mixed with the Nafion®/isopropanol solution at the initial step. The cross-section area of the electrode on which the catalyst–support 1:1 (w/w) mixture was deposited (geometrical area) was 0.07 cm².

2.3. Electrochemical experiments

2.3.1. Experimental apparatus

The RDE studies were carried out at 25 °C, in a conventional electrochemical cell with a water jacket, with three compartments for the work, counter and reference electrode, respectively. A mercury sulfate electrode (Hg/Hg_2SO_4/0.5 M H_2SO_4; abbreviated as MSE) was used as reference (MSE = 0.680 V (NHE), however, the potential values reported are referred to the normal hydrogen electrode (NHE); a carbon cloth was used as counter electrode. The 0.5 M H_2SO_4 electrolyte was prepared with 98% sulfuric acid (J. T. Baker) and deionized water (18.2 MΩ cm). A potentiostat/galvanostat (Princeton Applied Research, model 263A) and a PC with Echem-M270 software were used for the electrochemical measurements. A Radiometer Analytical BM-EDI101 glassy carbon rotating disk electrode (with a CTV101 speed control unit) was used for the voltammetry studies.

2.3.2. Electrochemical methods

2.3.2.1. Cyclic voltammetry.
Cyclic voltammetry (CV) experiments were done to clean, activate and characterize the electrode surface for both reactions studied (ORR and HOR). The electrode was purged with nitrogen (Praxair, ultra high purity) for 30 min before each CV measurement; then it was subjected to 40 potential sweeps between 0.0 and 1.03 V (NHE), at a 20 mV s^{-1} scan rate (stabilization was usually reached after 20 potential sweeps). The open circuit potential of the electrode in the N_2 saturated electrolyte ($E_{OC}^{N_2}$) was measured at the end of each experiment. In the case of the studies of Pt/Vulcan® electrodes, performed for reference, the potential sweeps were done in the 0.0–1.58 V (NHE) range, at a 50 mV s^{-1} rate. As for the hydrogen oxidation reaction in the presence of carbon monoxide, the same procedure was followed, however, after the first 40 potential sweeps, the electrolyte was saturated with carbon monoxide (Praxair, 99.5%) for 10 min; CV curves were then obtained after 5 potential sweeps also in the 0.0–1.03 V (NHE) range, at a 20 mV s^{-1} scan rate for the new materials, and in the 0.0–1.58 V (NHE) range, at a 50 mV s^{-1} rate for Pt/Vulcan®.

2.3.2.2. Hydrogen oxidation reaction.
Linear sweep voltammetry (LSV) was used to study the HOR on the new materials and on Pt/Vulcan® (as reference), in the absence and presence of carbon monoxide. The electrode was saturated with H_2 (Praxair, ultra high purity) for 15 min before each LSV measurement. The open circuit potential ($E_{OC}^{H_2}$ and $E_{OC}^{H_2/CO}$) was measured for each catalyst in the absence and presence of CO. Current–potential curves were obtained in the $E_{OC}^{H_2}$ to 680 mV (NHE) and $E_{OC}^{H_2/CO}$ to 680 mV (NHE) ranges, respectively, at a 10 mV s^{-1} scan rate. The rotation rates ranged from 100 to 3000 rpm. Measurements were performed at least three times for each material.

2.3.2.3. Oxygen reduction reaction.
LSV measurements were performed to study the oxygen reduction reaction on the new materials and on Pt/Vulcan® (as reference). The electrolyte was saturated with O_2 (Praxair, ultra high purity) for 15 min. The open circuit potential ($E_{OC}^{O_2}$) was measured for each catalyst.
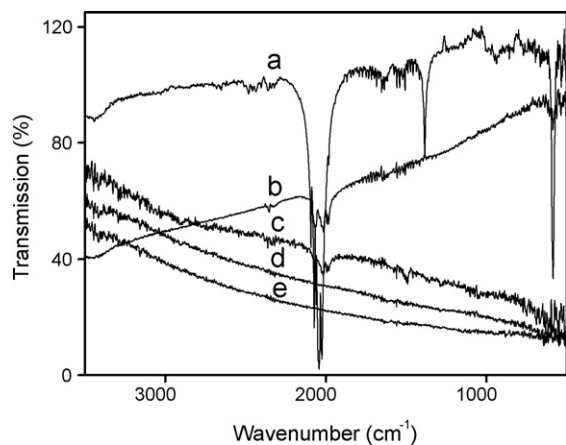
Fig. 1. FT-IR spectra of (a) the $Os_3(CO)_{12}$, and (b) $Os_3(CO)_{12}$/Vulcan® precursors. Representative FT-IR spectra of (c) the materials prepared in N_2 from the $Os_3(CO)_{12}$/Vulcan® precursor, at 120 °C; (d) the catalysts synthesized from $Os_3(CO)_{12}$/Vulcan® in the absence of solvents, at 180–320 °C; (e) the materials prepared in *n*-octane.
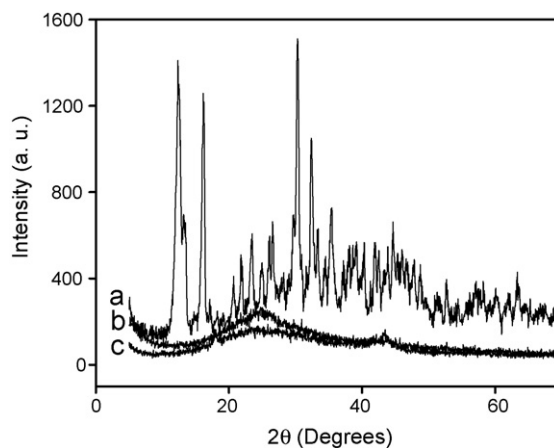

Fig. 2. (a) X-ray diffraction pattern of $Os_3(CO)_{12}$; (b) representative XRD pattern of the materials obtained from $Os_3(CO)_{12}$/Vulcan® in the absence of solvents, at 180–320 °C; (c) representative XRD pattern of the electrocatalysts prepared in *n*-octane.
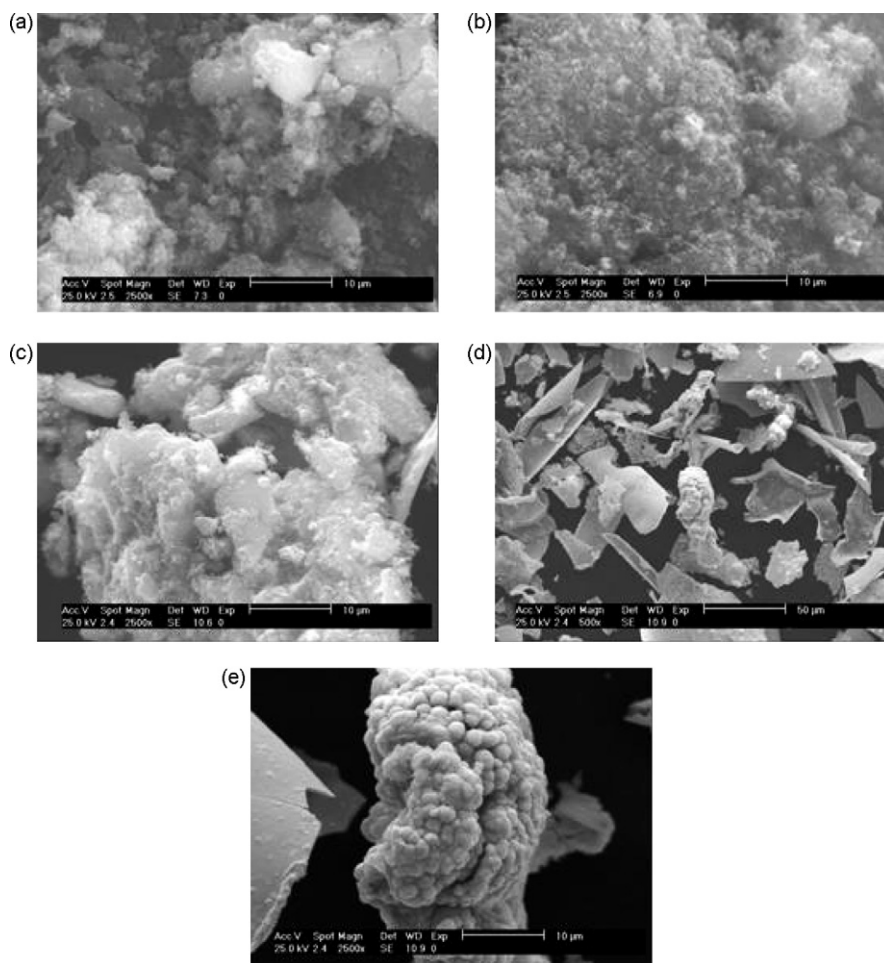

Fig. 3. Scanning electron micrographs of the electrocatalysts prepared with the following *precursor/conditions*: (a) $Os_3(CO)_{12}$–Vulcan®/N_2/320 °C/7 h (2500×); (b) $Os_3(CO)_{12}$–Vulcan®/N_2/320 °C/5 h (2500×); (c) $Os_3(CO)_{12}$–Vulcan®/*n*-octane/30 h (2500×); (d) and (e) $Os_3(CO)_{12}$/*n*-octane/72 h, at a 500× and 2500× magnification, respectively.

Current–potential curves were obtained in the $E_{OC}^{O_2}$ to 0.0 mV (NHE) range, at a 5 mV s^{-1} rate. The rotation rates ranged from 100 to 1600 rpm. Measurements were performed at least three times for each material.

3. Results and discussion

3.1. Structural characterization

Fig. 1 shows the FT-IR spectra of both precursors, $Os_3(CO)_{12}$ and $Os_3(CO)_{12}$/Vulcan®, as well as representative spectra of the materials prepared in the absence of solvents (in N_2) and in *n*-octane. The two precursors (Figs. 1a and b) show the well known group of carbonyl stretching bands around 2040 cm^{-1}, although they are much less intense in the case of $Os_3(CO)_{12}$/Vulcan®, due to the dissolution of the carbonyl cluster in the nano-sized carbon powder; the bands around 560 cm^{-1} have been assigned to carbonyl deformation modes, $\delta_{M\text{-}CO}$ [17]. All the materials prepared in N_2 from the $Os_3(CO)_{12}$/Vulcan® precursor, at the lowest pyrolysis temperature, *i.e.* 120 °C, show a group of weak υ_{CO} bands about 2020 cm^{-1} (Fig. 1c, as a representative example), which indicates that carbonyl groups are still present in
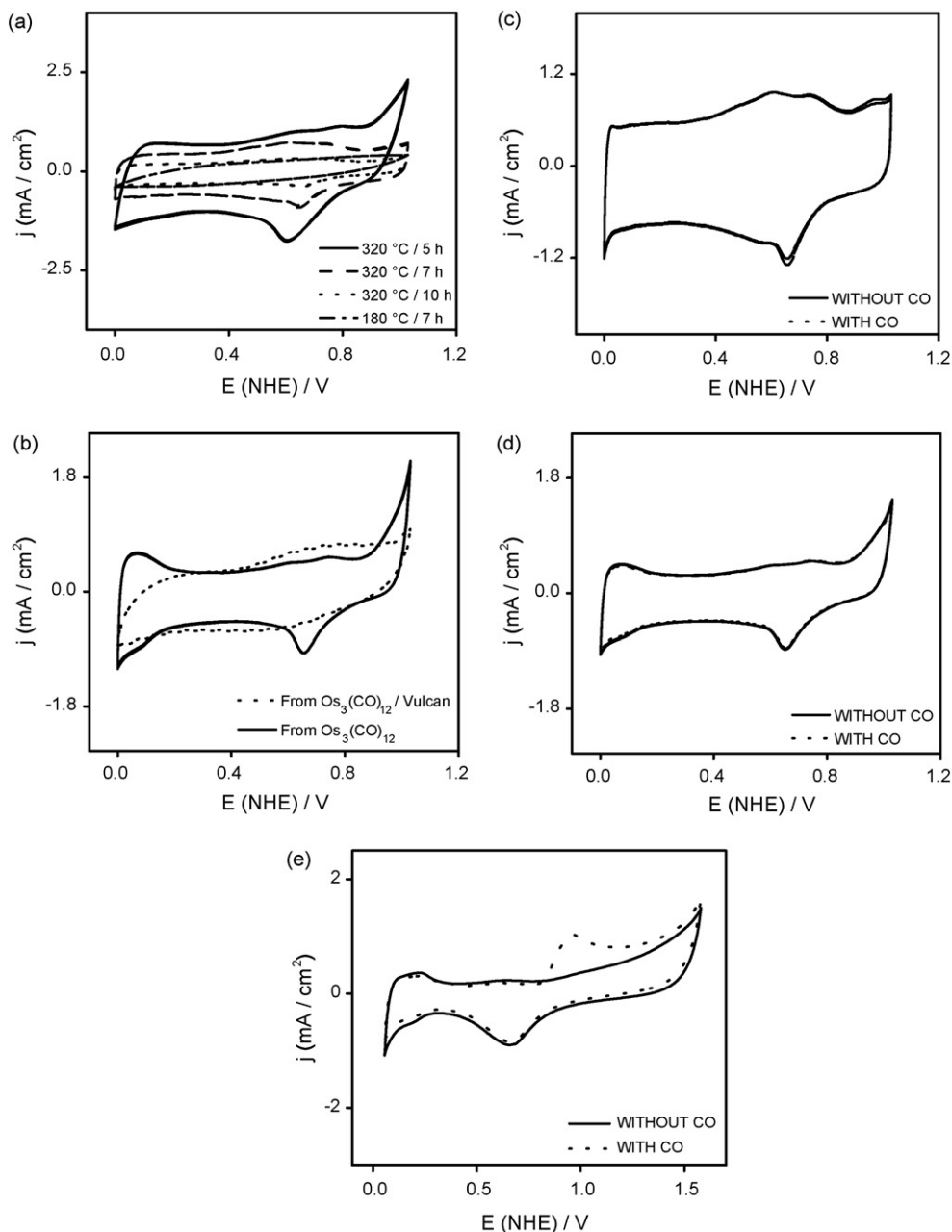

Fig. 4. Cyclic voltammograms for the electrocatalysts synthesized: (a) from $Os_3(CO)_{12}$/Vulcan® in N_2, at 180 °C (7 h) and 320 °C (5, 7 and 10 h); (b) from $Os_3(CO)_{12}$/Vulcan® for 30 h, and from $Os_3(CO)_{12}$ for 72 h, in *n*-octane. (c) and (d) *Representative* voltammograms *in the presence of CO* of the materials synthesized in the absence of solvents and in *n*-octane, respectively (the corresponding voltammograms in the absence of CO have been included for comparison). In all cases, the electrolyte was 0.5 M H_2SO_4 and the sweep rate 20 mV s^{-1}; (e) cyclic voltammograms of Pt/Vulcan® in the absence and presence of CO; the electrolyte was 0.5 M H_2SO_4 and the sweep rate 50 mV s^{-1}.

these products (although the intensity of such bands decreases with reaction time); the species formed are probably larger osmium clusters, possibly in the Os_5–Os_8 atom range [18]. In contrast, the stretching carbonyl bands are absent in the spectra of the materials prepared at higher temperatures (180–320 °C; Fig. 1d as representative example), as well as in those of the catalysts prepared in n-octane (Fig. 1e as representative example); in such cases, a virtually complete decarbonylation of the precursors is assumed. This is confirmed by the corresponding XRD patterns (Fig. 2; the pattern of $Os_3(CO)_{12}$ was included as reference, Fig. 2a), since a broad peak is obtained in the position ($2\theta \sim 43.3°$) of the most intense diffraction peak of metallic osmium, for both kinds of materials (Fig. 2b and c); a broad and intense signal centered at $2\theta \sim 24°$ is attributed to the Vulcan® support [19]. The broadness of the Os diffraction peak is indicative of the small size of the metal particles; this was confirmed by calculations based on the full width at half maximum (FWHM) of the peak, using the Scherrer formula [20]; the results indicated an average osmium particle size of 5 nm for these materials. In summary, the products synthesized at temperatures >120 °C basically consist of osmium nanoparticles, while the materials prepared at 120 °C are most likely carbonyl clusters, presumably larger than the Os_3 precursor (further characterization of such compounds is currently underway).

Fig. 3 shows representative SEM images of the most active materials for both reactions. These images show clusters of different size and a sponge-like morphology for the electrocatalysts prepared from $Os_3(CO)_{12}$/Vulcan® in both reaction media (Fig. 3a–c); the materials synthesized from $Os_3(CO)_{12}$, on the other hand, show a more irregular morphology, with both smooth and relatively rough surface clusters, as observed in Fig. 3d; a detail of the latter, with its grape cluster-like microstructure, is shown in Fig. 3e.

3.2. Electrochemical characterization

3.2.1. Cyclic voltammetry

Fig. 4 shows the cyclic voltammograms of the materials with the highest electroactivity for the ORR and/or HOR, according to the kinetic parameters (Section 3.2.2), namely, those prepared from $Os_3(CO)_{12}$/Vulcan® in N_2, at 180 °C (7 h) and 320 °C (5, 7 and 10 h), Fig. 4a, as well as those synthesized in n-octane, from $Os_3(CO)_{12}$/Vulcan® for 30 h, and from $Os_3(CO)_{12}$ for 72 h, Fig. 4b. Representative voltammograms of the electrocatalysts in the presence of CO are shown in Fig. 4c and d, for the materials synthesized in the absence of solvents and in n-octane, respectively; the cyclic voltammogram of a Pt/Vulcan® electrode has been included as reference, Fig. 4e. It was observed that the voltammograms did not change with cycling time, but remained stable for more than 1 h.

The cyclic voltammograms in Fig. 4a and b show anodic–cathodic peaks in the 0.5–0.85 V (NHE) region, which
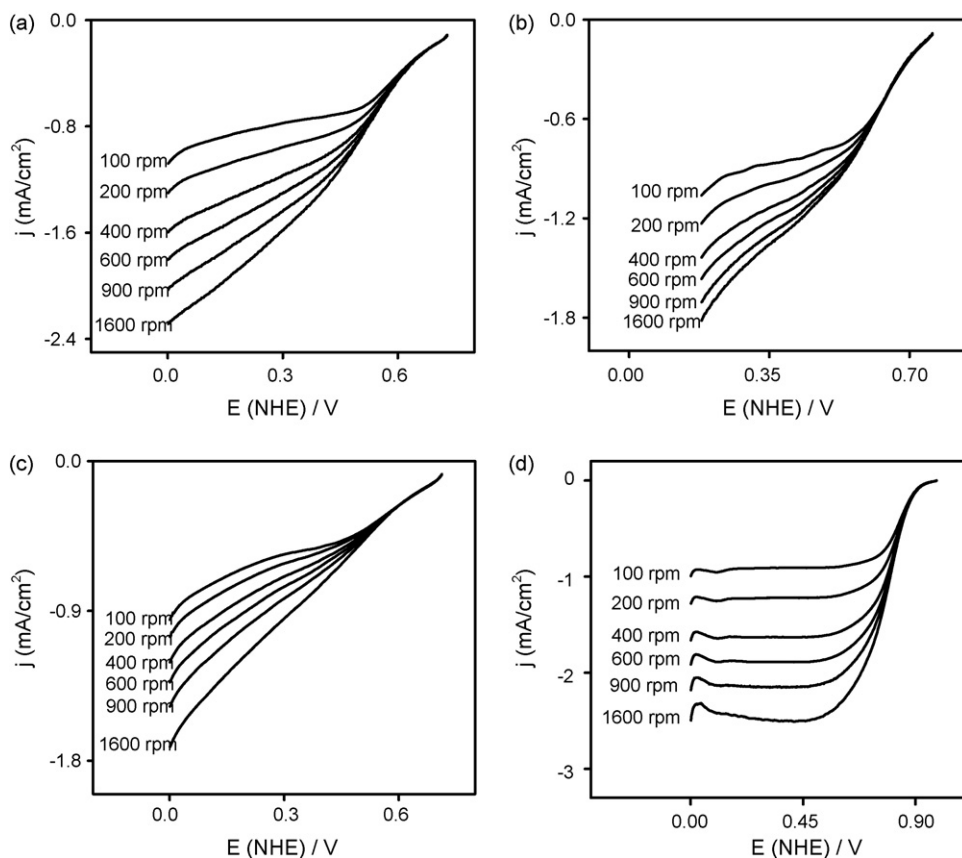

Fig. 5. ORR rotating disk electrode current–potential curves for the materials prepared with the following *precursor/conditions*: (a) $Os_3(CO)_{12}$–Vulcan®/N_2/320 °C/5 h; (b) $Os_3(CO)_{12}$–Vulcan®/n-octane/30 h; (c) $Os_3(CO)_{12}$/n-octane/72 h; (d) ORR rotating disk electrode current–potential curves for Pt/Vulcan®. In all cases the electrolyte was 0.5 M H_2SO_4 and the sweep rate 5 mV s^{-1}.
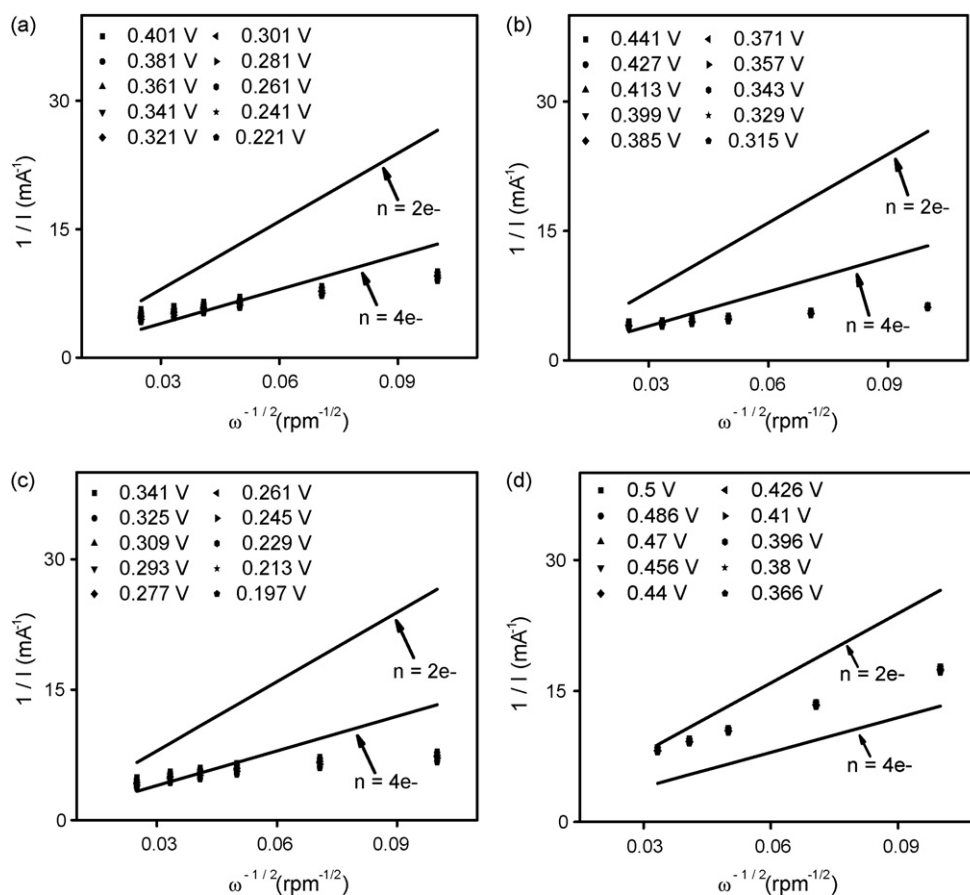
Fig. 6. Experimental Koutecky–Levich plots for the electrocatalysts prepared with the following *precursor/conditions*: (a) $Os_3(CO)_{12}$–Vulcan®/N_2/320 °C/5 h; (b) $Os_3(CO)_{12}$–Vulcan®/n-octane/30 h; (c) $Os_3(CO)_{12}$/n-octane/72 h; (d) experimental Koutecky–Levich plots for Pt/Vulcan®. In all cases, the plots are compared with those calculated for two- and four-electron oxygen reduction processes.

can be possibly ascribed to the oxidation–reduction process of the osmium metal particles, as is observed for platinum [21]. Hydrogen and oxygen evolution zones in the cathodic 0.0–0.2 V (NHE) and anodic 0.85–1.0 V (NHE) region, respectively, are observed in both cases as well. On the other hand, as can be clearly observed in Fig. 4c and d, the electrochemical behavior of all these materials is practically unaffected by the presence of carbon monoxide, the oxidation peak of the latter not being observed at ∼0.78 V (NHE); in contrast, the peak is clearly defined in the cyclic voltammogram of platinum, Fig. 4e.

3.2.2. Linear sweep voltammetry

3.2.2.1. Oxygen reduction reaction (ORR). Fig. 5 shows the polarization curves of the materials that exhibit the highest electrocatalytic activity for the oxygen reduction reaction, *i.e.* those synthesized in N_2 at 320 °C (5 h) and the two materials prepared in n-octane; the current-potential curves of Pt/Vulcan® have been included as reference as well. It can be seen that the materials synthesized in the organic solvent show lower current densities for the ORR than that prepared by the solvent-free route; the j values of the latter are similar to the experimental values of platinum. The electrocatalyst prepared by the solvent-free method, together with that prepared from the $Os_3(CO)_{12}$/Vulcan® precursor in n-octane, exhibit a bet-

ter defined diffusion plateau than the material obtained from $Os_3(CO)_{12}$ in the same solvent. The inclination of the curves with the rotation speed has been previously observed for catalyzed irreversible electrode processes [22]. Fig. 6 shows the corresponding Koutecky–Levich plots for the electrocatalysts described above. As is known, the ORR can occur by two different pathways: one – involving four electrons – in which O_2 is reduced directly to H_2O at the electrode solid/solution interface, or a two-electron process, which involves the formation of hydrogen peroxide and its subsequent reduction to water [23]. As the kinetics of the ORR is concerned, an electrocatalyst that performs the reaction directly, via four electrons, is clearly more efficient. The Koutecky–Levich theoretical plots for two- and four-electron processes can be obtained according to the following equation:

$$\frac{1}{B} = \frac{1}{0.62} n A F v^{-1/6} D_{O_2}^{2/3} C_{O_2} \tag{1}$$

where $1/B$ is the Koutecky–Levich slope, n the number of electrons involved, A the geometrical area of the electrode and F the Faraday constant; the values of the electrolyte kinematic viscosity (v) and the oxygen diffusion coefficient (D) and concentration in the electrolyte (C) were considered as follows: $v = 0.01 \, \text{cm}^2 \, \text{s}^{-1}$, $D_{O_2} = 1.4 \times 10^{-5} \, \text{cm}^2 \, \text{s}^{-1}$ and $C_{O_2} = 1.1 \times 10^{-6} \, \text{mol cm}^{-3}$ [24]. A comparison of the theoretical and
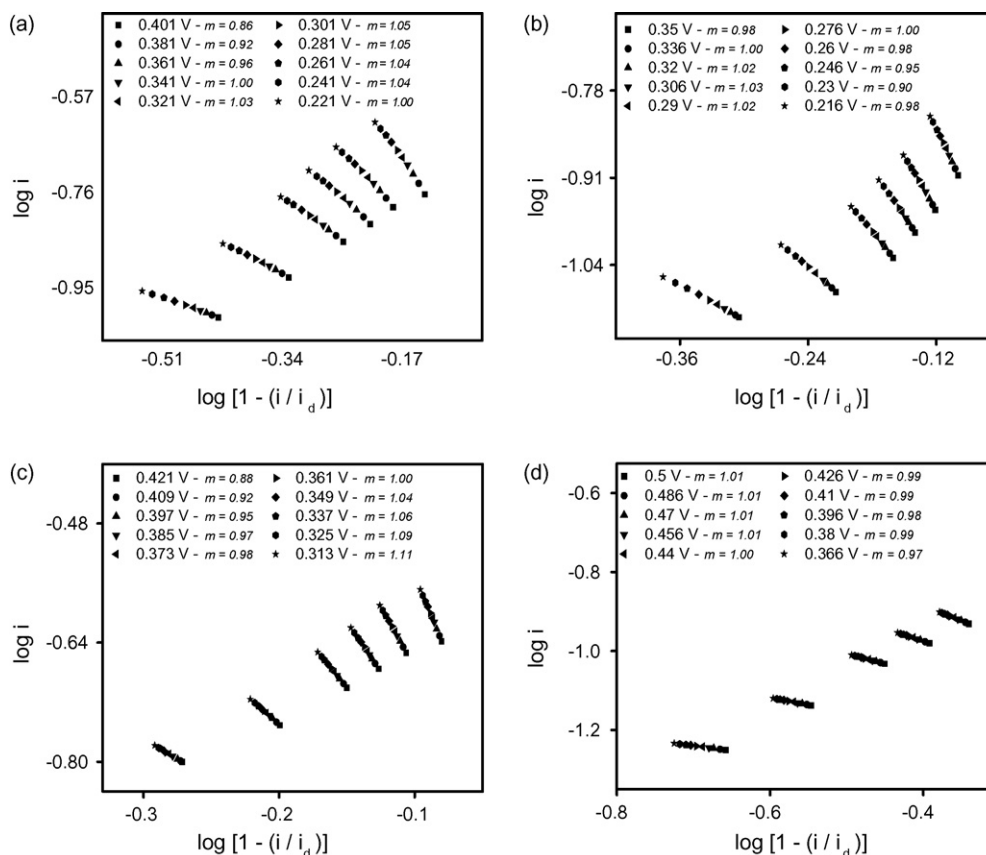
Fig. 7. $\log i$ vs. $\log[1-(i/i_d)]$ plots for several rotation rates at a given potential for the electrocatalysts prepared with the following *precursor/conditions*: (a) $Os_3(CO)_{12}$–Vulcan®/N_2/320 °C/5 h; (b) $Os_3(CO)_{12}$–Vulcan®/*n*-octane/30 h; (c) $Os_3(CO)_{12}$/*n*-octane/72 h; (d) $\log i$ vs. $\log[1-(i/i_d)]$ plots for Pt/Vulcan®. The reaction order, m, is shown for each potential value in the calculation range.

experimental plots shows that the latter are closer to the plots calculated for a four-electron process, than they are to those of a two-electron route, as is observed for platinum. Hence, the new electrocatalysts most likely reduce the oxygen molecules directly to water.

The reaction order [25], m, calculated from the slope of the $\log i$ versus $\log[1-(i/i_d)]$ plots (where i_d is the diffusion current) for several rotation rates at a given potential (Fig. 7; average values in Table 1), is virtually *one* with respect to dissolved O_2 in the 0.5 M H_2SO_4 electrolyte for all materials (Fig. 7a–c); very similar values were calculated for Pt/Vulcan® (Fig. 7d).

Normally, the kinetic current (i_k) values obtained from the extrapolation of the Koutecky–Levich plots are used to build the Tafel curves ($\log i_k$ versus E), from which the kinetic parameters, *i.e.* the Tafel slope (b), the exchange current density (j_0) and the

transfer coefficient (α), can be obtained. However, highly precise results may not be obtained due to inevitable experimental variations in the preparation of the electrode; for this reason, the current–potential curves were corrected by the procedure described by Gojkovic et al. [26]; these curves, in turn, yielded the mass corrected Tafel plots, Fig. 8, which allowed the calculation of the kinetic parameters presented in Table 1; the values for platinum are shown as well. Most notably, the exchange current density values of these osmium materials (5.5×10^{-5} to 8.5×10^{-4} mA cm^{-2}) are higher, by one or two orders of magnitude, than those of platinum (4×10^{-6} mA cm^{-2}) in all cases.

As regards the Tafel slope, a parameter related to the reaction mechanism [27], the experimental value of 118 mV dec^{-1} for platinum is considerably smaller than those for the novel materi-

Table 1
Open circuit potential and average kinetic parameters of the novel electrocatalysts and Pt/Vulcan® for the oxygen reduction reaction (ORR)

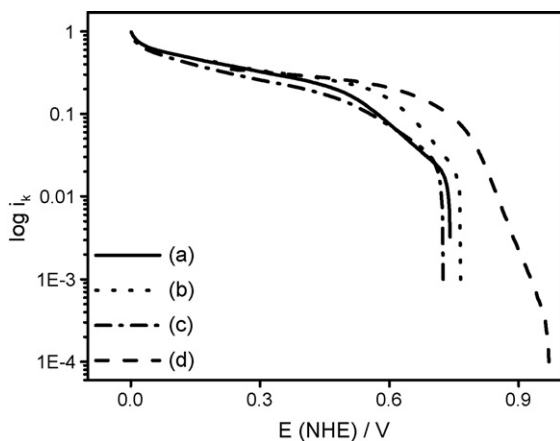| Electrocatalyst (precursor/conditions)	E_{OC} (V NHE)	m	b (mV dec^{-1})	α	j_0 (mA cm^{-2})
$Os_3(CO)_{12}$–Vulcan®/N_2, 320 °C, 5 h	0.743	1.004	233	0.2584	7.31×10^{-4}
$Os_3(CO)_{12}$/*n*-octane, 72 h	0.722	0.980	161	0.3728	5.47×10^{-5}
$Os_3(CO)_{12}$–Vulcan®/*n*-octane, 30 h	0.762	1.005	230	0.2709	8.52×10^{-4}
Pt/Vulcan®	0.974	0.996	118	0.5084	1.41×10^{-6}

Fig. 8. ORR mass-corrected Tafel plots for the electrocatalysts prepared with the following *precursor/conditions*: (a) $Os_3(CO)_{12}$–Vulcan®/N_2/320 °C/5 h; (b) $Os_3(CO)_{12}$–Vulcan®/*n*-octane/30 h; (c) $Os_3(CO)_{12}$/*n*-octane/72 h; (d) ORR mass-corrected Tafel plots for Pt/Vulcan®.

als (Table 1); such a difference might be regarded as suggestive of considerably different ORR mechanisms in these osmium materials.

In summary, the exchange current density values, as well as the Koutecky–Levich results (suggestive of a direct reduction process), are consistent with a relatively high electrocatalytic activity of these Os materials for the oxygen reduction reaction.

3.2.2.2. Hydrogen oxidation reaction. The materials that showed a favorable open circuit potential value ($E_{OC}^{H_2}$) to perform the HOR were the following: (a) those prepared from $Os_3(CO)_{12}$/Vulcan® in N_2 atmosphere, at 180 °C/7 h, 320 °C/5 h, 320 °C/7 h and 320 °C/10 h; (b) both materials synthesized in *n*-octane (from $Os_3(CO)_{12}$ and from $Os_3(CO)_{12}$/Vulcan®); the latter even in the presence of CO. Fig. 9 shows the polarization curves of the above materials and of Pt/Vulcan® as reference. An important observation is the fact that the current density of the materials prepared in N_2 at 320 °C increases with reaction time, the catalyst with the highest current density ($\sim$0.39 mA cm^{-2}) being that of a 10 h reaction time (Fig. 9a); on the other hand, the material prepared in the same atmosphere at 180 °C, for 7 h, exhibited the lowest current density, $\sim$0.26 mA cm^{-2} (Fig. 9a). As for the catalysts synthesized in the organic solvent, that prepared from $Os_3(CO)_{12}$ shows higher current density values than the material prepared from the $Os_3(CO)_{12}$/Vulcan® precursor (Fig. 9b and c).

In the case of the HOR in the presence of CO, the two electrocatalysts prepared in *n*-octane show a similar behavior to that exhibited in its absence (Fig. 9b and c), *i.e.* they are *tolerant* to carbon monoxide to some extent, an important advantageous property when compared to platinum, whose current density drops to zero when subjected to the presence of CO (Fig. 9d). The current density decrease observed for the Os electrocatalysts in the presence of CO could be accounted for, at
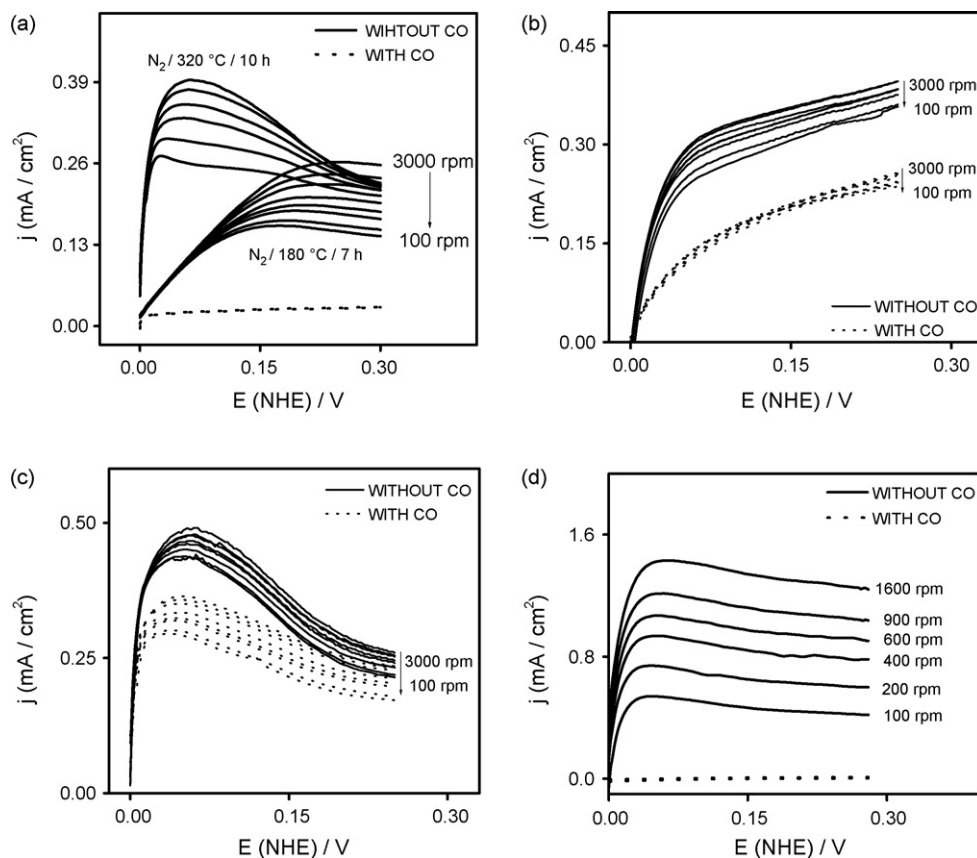

Fig. 9. HOR rotating disk electrode current–potential curves for the materials prepared with the following *precursor/conditions*: (a) $Os_3(CO)_{12}$–Vulcan®/N_2/180 °C/7 h and $Os_3(CO)_{12}$–Vulcan®/N_2/320 °C/10 h; (b) $Os_3(CO)_{12}$–Vulcan®/*n*-octane/30 h; (c) $Os_3(CO)_{12}$/*n*-octane/72 h; (d) HOR rotating disk electrode current–potential curves for Pt/Vulcan®. The electrolyte was 0.5 M H_2SO_4 and the sweep rate 10 mV s^{-1}.
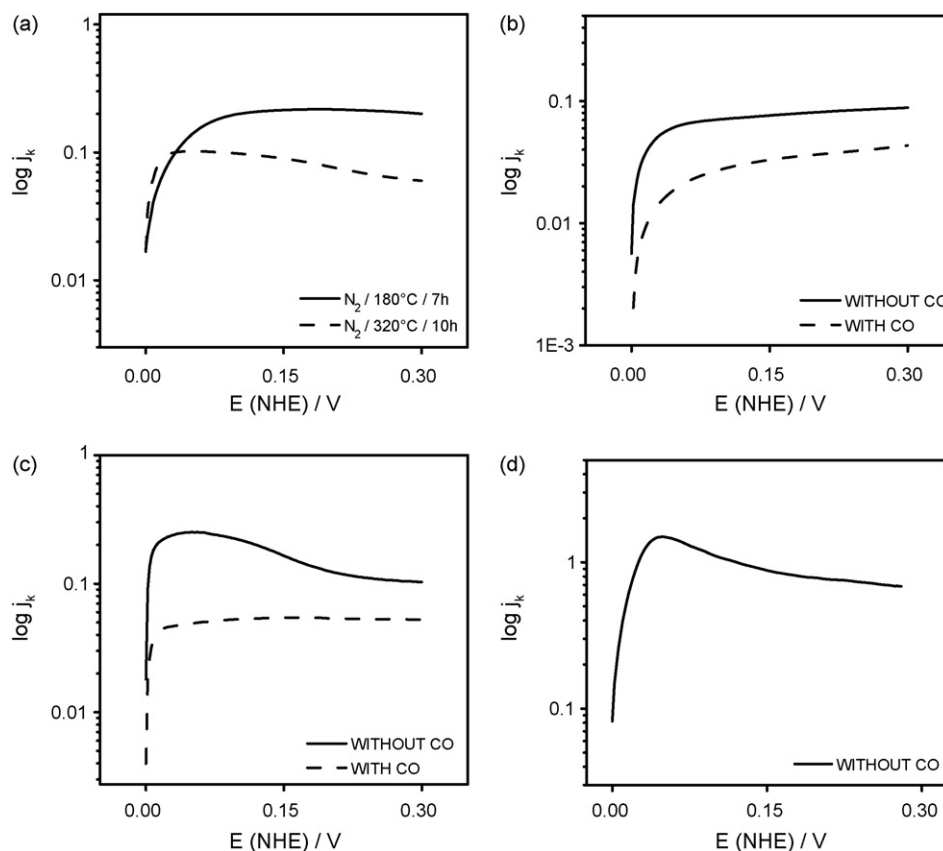
Fig. 10. HOR mass-corrected Tafel plots for the electrocatalysts prepared with the following *precursor/conditions*: (a) $Os_3(CO)_{12}$–Vulcan®/N_2/180 °C/7 h and $Os_3(CO)_{12}$–Vulcan®/N_2/320 °C/10 h; (b) $Os_3(CO)_{12}$–Vulcan®/*n*-octane/30 h; (c) $Os_3(CO)_{12}$/*n*-octane/72 h; (d) HOR mass-corrected Tafel plots for Pt/Vulcan®.

least partially, by changes in the H_2 concentration and diffusion coefficient when the carbon monoxide gas is present in the electrolyte.

On the other hand, the electrocatalysts synthesized by pyrolysis in N_2 are not capable to perform the HOR in the presence of CO, at 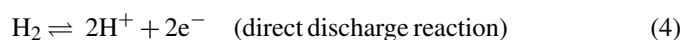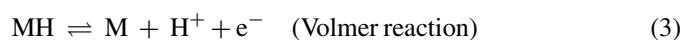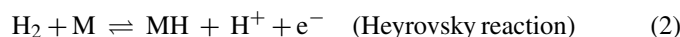least under the present experimental conditions, as inferred from the severe current density drop observed in Fig. 9a. However, it is suggested that if lower concentrations of CO were used, of the order of parts per million (ppm), as in most reports [1,28,29], some tolerance could be possibly observed (in the present work, *pure* CO was bubbled into the electrochemical cell for 10 min, immediately before the LSV measurements).

Table 2
Open circuit potential and average kinetic parameters of the novel electrocatalysts and Pt/Vulcan® for the hydrogen oxidation reaction (HOR) in the absence and presence of carbon moxide (CO)

Electrocatalyst (precursor/conditions)	CO	E_{OC} (V NHE)	b (mV dec^{-1})	j_0 (mA cm^{-2})	α
$Os_3(CO)_{12}$–Vulcan®/N_2, 180 °C, 7 h	Without	0.0	43	0.0311	0.4158
	With	0.0	–	–	–
$Os_3(CO)_{12}$–Vulcan®/N_2, 320 °C, 5 h	Without	0.0	43	0.0355	0.4129
	With	0.0	–	–	–
$Os_3(CO)_{12}$–Vulcan®/N_2, 320 °C, 7 h	Without	0.0	43	0.0365	0.4303
	With	0.0	–	–	–
$Os_3(CO)_{12}$–Vulcan®/N_2, 320 °C, 10 h	Without	0.0	48	0.0199	0.25
	With	0.0	–	–	–
$Os_3(CO)_{12}$/*n*-octane, 72 h	Without	0.0	39	0.0780	0.5522
	With	0.0	44	0.0837	0.3664
$Os_3(CO)_{12}$–Vulcan®/*n*-octane, 30 h	Without	0.0	32	0.0378	0.9052
	With	0.0	32	0.0350	0.8465
Pt/Vulcan®	Without	0.0	28	0.4748	1.0
	With	0.0	–	–	–

The kinetic parameters of the above materials, *i.e.* the Tafel slope (*b*), the exchange current density (j_0) and the transfer coefficient (α), were calculated from the corresponding mass-corrected Tafel plots, representative examples of which are shown in Fig. 10; the results have been summarized in Table 2, along with those of Pt/Vulcan® as reference. If the calculated Tafel slopes (*b*) could be associated with the reaction pathways proposed by Mello and Ticianelli for the HOR [30], the present materials would follow a Heyrovsky/Volmer type mechanism (Eqs. (2) and (3)), for which $b = 40$ mV dec^{-1}, with the exception of the catalyst prepared from $Os_3(CO)_{12}$/Vulcan® in *n*-octane, which, under the same considerations, could possibly perform the hydrogen oxidation through a direct discharge mechanism (Eq. (4)), associated with a Tafel slope of 30 mV dec^{-1}.

$$H_2 + M \rightleftharpoons MH + H^+ + e^- \quad \text{(Heyrovsky reaction)} \quad (2)$$

$$MH \rightleftharpoons M + H^+ + e^- \quad \text{(Volmer reaction)} \quad (3)$$

$$H_2 \rightleftharpoons 2H^+ + 2e^- \quad \text{(direct discharge reaction)} \quad (4)$$

Although the exchange current density values of the new materials are lower than those obtained for platinum (0.47 mA cm^{-2}), the significant CO tolerance exhibited by the new osmium materials prepared in *n*-octane is a clear advantage over Pt catalysts; in fact, the j_0 values of the such two electrocatalysts are very similar in the absence and presence of CO (Table 2).

4. Conclusions

Novel Os-based electrocatalysts for the ORR and/or HOR have been prepared in this work. While most of them basically consist of osmium metal nanoparticles, their electrocatalytic properties are strongly influenced by the precursor and reaction medium employed. Six of the novel electrocatalysts can perform the hydrogen oxidation reaction, and three of them [those synthesized in (*a*) N_2/320 °C/5 h, and in *n*-octane from (*b*) $Os_3(CO)_{12}$/Vulcan® and (*c*) $Os_3(CO)_{12}$], also perform the oxygen reduction reaction, most likely following a direct, four-electron pathway, and with exchange current densities one or two orders of magnitude higher than that of platinum. A very important characteristic of the two electrocatalysts prepared in *n*-octane is that they are significantly tolerant to carbon monoxide; this is a clear advantage over platinum catalysts – which are easily deactivated even by traces of CO – which could open the possibility of using reforming hydrogen, instead of highly pure H_2, as fuel feed in PEFC, thus lowering their operation cost. Hence, these materials can be considered as potential candidates to be used as anodes and/or cathodes in polymer electrolyte fuel cells.

Acknowledgements

References

[1] T. Ioroi, N. Fujiwara, Z. Siroma, K. Yasuda, Y. Miyazaki, Electrochem. Commun. 4 (2002) 442–446.
[2] C.E. Thomas, B.D. James, F.D. Lomas Jr., I.F. Kuhn Jr., Int. J. Hydrogen Energy 25 (2000) 551–567.
[3] W. Wiese, B. Emonts, R. Peters, J. Power Sources 84 (1999) 187–193.
[4] O. Korotkikh, R. Farrauto, Catal. Today 62 (2000) 249–254.
[5] V. Le Rhun, E. Garnier, S. Pronier, N. Alonso-Vante, Electrochem. Commun. 2 (2000) 475–479.
[6] M. Bron, P. Bogdanoff, S. Fiechter, M. Hilgendorff, J. Radnik, I. Dorbandt, H. Schulenburg, H. Tributsch, J. Electroanal. Chem. 517 (2001) 85–94.
[7] R.H. Castellanos, E. Borja-Arco, A. Altamirano-Gutiérrez, R. Ortega-Borges, Y. Meas, O. Jiménez-Sandoval, J. New Mater. Electrochem. Syst. 8 (2005) 69–75.
[8] S. Marcotte, D. Villers, N. Guillet, L. Roué, J.P. Dodelet, Electrochim. Acta 50 (2004) 179–188.
[9] G. Faubert, R. Côté, D. Guay, J.P. Dodelet, G. Dénès, C. Poleunis, P. Bertrand, Electrochim. Acta 43 (1998) 1969–1984.
[10] G. Faubert, R. Côté, D. Guay, J.P. Dodelet, G. Dénès, P. Bertrand, Electrochim. Acta 43 (1998) 341–353.
[11] M. Bron, P. Bogdanoff, S. Fiechter, H. Tributsch, J. Electroanal. Chem. 578 (2005) 339–344.
[12] E.I. Santiago, E.A. Ticianelli, Int. J. Hydrogen Energy 30 (2005) 159–165.
[13] S.H. Bonilla, C.F. Zinola, J. Rodríguez, V. Díaz, M. Ohanian, S. Martínez, B.F. Gianetti, J. Colloid Interf. Sci. 288 (2005) 377–386.
[14] R.H. Castellanos, R. Rivera-Noriega, O. Solorza-Feria, J. New Mater. Electrochem. Syst. 2 (1999) 85–88.
[15] R.H. Castellanos, A.L. Ocampo, J. Moreira-Acosta, P.J. Sebastian, Int. J. Hydrogen Energy 26 (2001) 1301–1306.
[16] R.H. Castellanos, A.L. Ocampo, P.J. Sebastian, J. New Mater. Electrochem. Syst. 5 (2002) 83–90.
[17] C.E. Anson, U.A. Jayasooriya, Spectrochim. Acta 46A (1990) 861–869.
[18] F.A. Cotton, G. Wilkinson, Advanced Inorganic Chemistry, 4th ed., Interscience Publishers, Chichester, 1998.
[19] A.K. Shukla, R.K. Raman, in: K.D. Kreuer, D.R. Clarke, M. Rühle, J.C. Bravman (Eds.), Annual Review of Materials Research, vol. 33, Annual Reviews, Palo Alto, 2003, p. 161.
[20] B.D. Cullity, Elements of X-ray Diffraction, 2nd ed., Addison–Wesley, Reading, 1978.
[21] K. Jambunathan, B.C. Shah, J.L. Hudson, A.C. Hillier, J. Electroanal. Chem. 500 (2001) 279–289.
[22] R. Jiang, D. Chu, J. Electrochem. Soc. 147 (2000) 4605–4609.
[23] K. Kinoshita, Electrochemical Oxygen Technology, John Wiley & Sons, Berkeley, 1992, pp. 19–40.
[24] A.L. Ocampo, R.H. Castellanos, P.J. Sebastian, J. New Mater. Electrochem. Syst. 5 (2002) 163–168.
[25] T. Jiang, G.M. Brisard, Electrochim. Acta 52 (2007) 4487–4496.
[26] S.L. Gojkovic, S.K. Zecevic, R.F. Savinell, J. Electrochem. Soc. 145 (1998) 3713–3720.
[27] D.B. Sepa, M.V. Vojnovic, A. Damjanovic, Electrochim. Acta 26 (1981) 781–793.
[28] E.I. Santiago, V.A. Paganin, M. do Carmo, E.R. Gonzalez, E.A. Ticianelli, J. Electroanal. Chem. 575 (2005) 53–60.
[29] L. Giorgi, A. Pozio, C. Bracchini, R. Giorgi, S. Turtù, J. Appl. Electrochem. 31 (2001) 325–334.
[30] R.M.Q. Mello, E.A. Ticianelli, Electrochim. Acta 42 (1997) 1031–1039.